JOURNAL OF MATERIALS RESEARCH AND TECHNOLOGY 2021;15:4993–5009

Available online at www.sciencedirect.com

jmr&t Journal of Materials Research and Technology

journal homepage: www.elsevier.com/locate/jmrt

Original Article

Synthesis, physico-mechanical properties, material processing, and math models of novel superior materials doped flake of carbon and colloid flake of carbon

Mehmet Serkan Kırgız [a,b], *André Gustavo de Sousa Galdino* [c,*], *John Kinuthia* [d], *Anwar Khitab* [e], *Muhammad Irfan Ul Hassan* [f], *Jamal Khatib* [g], *Hesham El Naggar* [h], *Carlos Thomas* [i], *Jahangir Mirza* [j], *Said Kenai* [k], *Tuan Anh Nguyen* [l], *Moncef Nehdi* [m], *Muhammad Syarif* [n], *Ahmed Ashteyat* [o], *Ravindran Gobinath* [p], *Ahmed Soliman* [q], *Trinity A. Tagbor* [r], *Manoj A. Kumbhalkar* [s], *Naraindas Bheel* [t], *Chandra Sekhar Tiwary* [u]

[a] Department of Architecture, Engineering Architecture Faculty, Nişantaşı University, İstanbul, 34398, Turkey
[b] Department of Architecture, Faculty of Engineering and Natural Sciences, İstanbul Sabahattin Zaim University, İstanbul 34303, Turkey
[c] Federal Institute of Education, Science and Technology of Espírito Santo, Av. Vitória, 1729, Jucutuquara, Vitória, ES, 29040-780, Brazil
[d] Advanced Materials Testing Centre (AMTeC), University of South Wales, United Kingdom
[e] Mirpur University of Science and Technology (MUST), Mirpur, 10250, AJ&K, Pakistan
[f] University of Engineering and Technology, Civil Engineering Department, Lahore, Pakistan
[g] Department of Civil and Environmental Engineering, Faculty of Engineering, Beirut Arab University, Lebanon
[h] Department of Civil and Environmental Engineering, Faculty of Engineering, Western University, London, ON, Canada
[i] LADICIM (Laboratory of Materials Science and Engineering), University of Cantabria, 39005, Santander, Spain
[j] Faculty of Civil and Environmental Engineering, York University, Toronto, Canada
[k] Geomaterials and Civil Engineering Laboratory, Civil Engineering Department, University of Blida1, Algeria
[l] Institute for Tropical Technology, Vietnam Academy of Science and Technology, Viet Nam
[m] Department of Civil and Environmental Engineering, Faculty of Engineering, Western University, 1151 Richmond St, London, ON, N6A 3K7, Canada
[n] Muhammadiyah Makassar University of Indonesia, IDN, Indonesia
[o] Department of Civil Engineering, The University of Jordan, Amman, 11942, Jordan
[p] SR Engineering College, Warangal, Telangana, 456, India
[q] Department of Building, Civil, and Environmental Engineering, Gina Cody School of Engineering and Computer Science, Concordia University, Montreal, Quebec, Canada
[r] CSIR-Institute of Industrial Research, P.O Box LG 57, Legon, Accra, Ghana
[s] Department of Mechanical Engineering, JSPM Narhe Technical Campus, Pune, 411041, India
[t] Department of Civil and Environmental Engineering, Universiti Teknologi PETRONAS, Bandar Seri Iskandar, Tronoh, Perak, 31750, Malaysia
[u] Metallurgical and Materials Engineering, Indian Institute of Technology, Kharagpur, West Bengal, 721302, India

* Corresponding author.
E-mail address: andregsg@ifes.edu.br (A.G.S. Galdino).

https://doi.org/10.1016/j.jmrt.2021.10.089

ARTICLE INFO

Article history:
Received 22 June 2021
Accepted 19 October 2021
Available online 30 October 2021

Keywords:
Flake of nano carbon
Colloid flake of carbon
Pulverized fuel ash
Mechanical properties
Physical properties
Durability

ABSTRACT

High performance colloid flake of carbon is gaining interest due importance in meeting the challenges of the globe. To make novel superior materials, the pulverized fuel ash-green adhesive based construction materials modified with the flake of carbon and the colloid flake of carbon were evaluated in view of synthesis, physico-mechanical properties, and material processing and models. For better understanding, such experimental samples as green adhesive plaster and green adhesive grout were made of the pulverized fuel ash of class C, the common adhesive, the flake of carbon, the colloid flake of carbon, fine sand, and the distilled water to compare with the structural material properties each other. The results of the adsorption spectra of optical atomic spectroscopy of the colloid flake carbon, the thickening-period of plaster, the spread and the consolidating level, the apparent unit volume mass, the apparent porosity, the apparent compacity, and the compressive stress of green grouts were reported in the research. It was concluded that the flake of carbon and the colloid flake of carbon led to important progress in the novel superior materials, e.g., accelerating of the thickening-period of plasters and increasing of the compressive stress of grouts.

1. Introduction

There is plenty of much issue based on non-renewable resources, e.g., supplying of coal, sustaining of coal quality, greenhouse gas emission (GHG) and reducing of fuel ash generated by power plant and super power plant, in energy manufacturing [1]. Adhesive material industry also encounters similar problem as energy industry being, e.g., raw material consuming, the GHG emission, and increasing in energy demand [2]. As a consequence of the popularity of two industries, the demand of reducing of fuel ash in the energy industry is intertwined with the demand of reducing of raw material consuming in the adhesive material industry [1,2]. Pulverized fuel ash and fly ash generated by energy industry have chemical composition and pozzolanic activity that allow them to be used in supplementary cementitious material (SCM) as artificial pozzolanic additive material and/or substitution material for adhesive industry [3,4]. Therefore, the use of these two wastes as raw materials for other applications could be very useful to give them a better destination. There are plenty of much articles that add the pulverized fuel ash to fabricate geopolymer concrete, geopolymerized mansory mortar, coal like material, light weight material for roads, and for soil stabilization [5–9]. Those efforts are known as the manufacturing of ecology-friendly adhesive and adhesive based material.

On the other hand, since the research efforts did not establish a kind of polymer bonding between hydroxides in conventional adhesive, the people were not considering those new adhesives and materials to use in the construction industry. Therefore, there is a necessity to develop the structure of polymer bonding in adhesive based material. In order to properly set up the bonding of polymer in the adhesive based material and react the pulverized fuel ash with adhesive based material to saturate the surplus content of calcium hydroxide ($Ca(OH)_2$) with its useful oxides, the flake of carbon and the colloid flake of carbon, which has a covalent bonding of carbon–carbon (C–C), for ecology-friendly adhesive based material as supplementary material could be a solution in the necessity in use [3,4,10].

Moreover, a number of comprehensive research demonstrates that there is plenty of much advantage of flake of carbon on the properties of mechanical, thermal, and durability of adhesive and adhesive based construction material [11–21]. Nevertheless; they did not compare differences between the effect of flake of carbon and the effect of colloid flake of carbon on the physico-mechanical properties of adhesive and adhesive based construction material. The working would explain the performance of flake of carbon and colloid flake of carbon on the physico-mechanical properties of adhesive and adhesive based construction material and also compare the differences between the effects as the working develops new adhesives and new construction materials.

The application field of ecology-friendly adhesive of pulverized fuel ash of class C doped flake of carbon and colloid flake of carbon includes some sections of construction below, but is not limited to: Floor screeding, Adhesive rendering, Paving slab base, Bricklaying grout, Foundation, Oil Well Adhesive, Heavy concrete work, Hydraulic adhesive based injection for retrofit of existing construction, Hydraulic adhesive based stucco for reinforced-concrete and masonry construction, Hydraulic adhesive based bedding grout for reinforced-concrete and masonry construction, Grout for regular purposes, Concrete for special purposes.

This work aimed to present the properties of conventional adhesive doped flake of carbon and new ecology-friendly adhesive doped flake of carbon, and conventional and ecology-friendly adhesive-based construction materials doped colloid flake of carbon-performance effect assessment (PEA) and to compare their properties each other. As there is no special technological specification and constructional properties for ecology-friendly adhesive and its application, this paper also fills the gap between the technological requirements and constructional properties for the sections of construction previously suggested.

2. Materials and methods

2.1. Materials

The ASTM type I adhesive, the flake of carbon, and the pulverized class Cfuel ash are constituent materials with micro- and nano-size particle to measure the effect of flake of carbon and colloid flake of carbon on the physico-mechanical properties of new ecology-friendly adhesive, superior plaster and grout in this working. Fig. 1 shows the constituent materials used for synthesis and samples of conventional and ecologic-friendly adhesive doped flake of carbon and fine sand of grout and deionized water and super plasticizer.

2.1.1. *Flake of carbon*

One of the most known resources for the flake of carbon is the geological form of natural graphite. Another major resource of it is the artificial form of graphite that needs heat between 2500 and 3000 °C in its manufacturing, it is used in the manufacturing of extremely pure material like computer screen [10]. The geological form of natural graphite is sorted in four subtitles such as the flake graphite, the amorphous graphite, the graphite occurred in the hydrothermal process, and the graphite melted from rocks and meteoroids [22]. The flake of carbon from graphite is also manufactured from two major resources as seen in Fig. 2.

Either the geological form of graphite or the artificial form of graphite composed of pure carbon because its flake includes 99.9% carbon [3,4,10]. Almost all the flake graphite occurred at external part of Earth today is formed at concurrent plate zones where organic-mac shale and limestone are exposed to the heat and pressure of local metamorphism. This is manufactured by schist, gneiss, and marble that make of very small crystals and leaves of graphite. The metamorphism

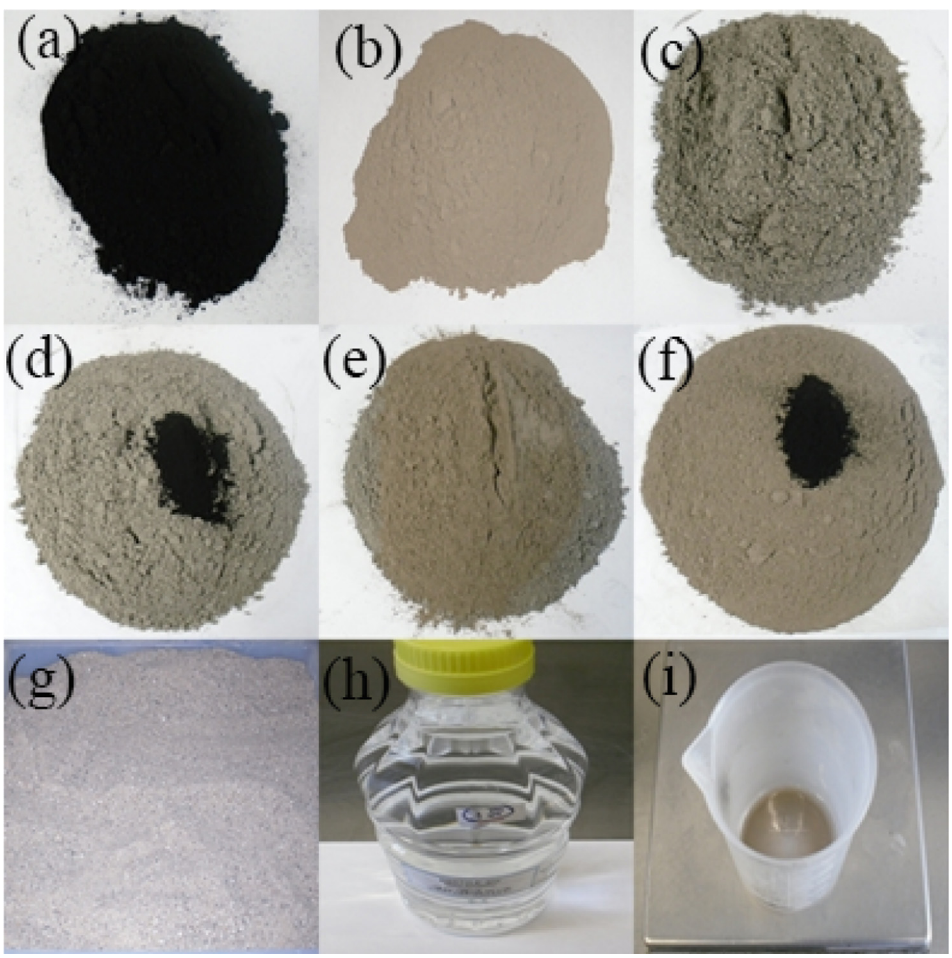

Fig. 1 – (a) Flake of carbon; (b) pulverized class C fuel ash; (c) ASTM type I adhesive; (d) ASTM type I adhesive doped flake of carbon; (e) the stack of 65% ASTM type I adhesive and 35% pulverized class C fuel ash (ecologic-friendly adhesive, and ecology-friendly adhesive doped flake of carbon); (f) standard fine sand for grout samples; (g) deionized water; and (h) sodium based super plasticizer.

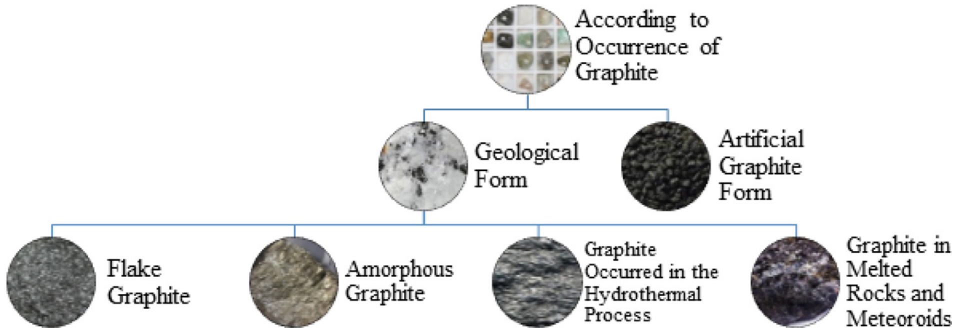

Fig. 2 – Origin of the flake of carbon.

of coal bed also generates the amorphous graphite. Natural material in coal bed mainly contains carbon and elements of oxygen, hydrogen, nitrogen, and sulfur. The heat treatment of metamorphism splits the organic molecules of coal, and evaporates the oxygen, hydrogen, nitrogen, and sulfur. In the process, the remaining is a nearly pure carbon element that is the crystalline mineral graphite described as the amorphous graphite [22]. Fig. 3 presents the sample of geological form of graphite and the sample of artificial form of graphite.

The hydrothermal process reaction of carbon compound generates the graphite occurred in the rock; it is very small amount of graphite form. This form of carbon-rich-graphite can be placed and stored in a narrow layer in association with hydrothermal minerals. Since it is deposited, it has a high degree of crystallinity, and that provides it a preferred material for much conductivity process. The graphite in melted rock and meteoroid is known as fundamental mineral to exist. It is called as tiny particle in basalt stream and syenite. It is also known to generate in pegmatite layer. Some iron meteoroids also compose of small amounts of graphite. The artificial graphite is generated with the burning of high-carbon content materials, such as petroleum coke and coal-tar pitch, in the temperature range of 2500–3000 °C. At the high temperature, all changeable mineral and a lot of metallic minerals are devastated in the raw material. The left graphite leaves link into the crystalline structure each other. Artificial graphite can contain over 99.9% of flake of carbon [23]. Table 1 lists the descriptive characteristic properties of flake of carbon.

2.1.2. *Colloid flake of carbon suspension*

The work uses the flake of carbon suspension liquid (water + sodium-based surfactant + flake of nano carbon) in order to measure its effect on the properties of ecology-friendly adhesive composite. This water+sodium-based surfactant+flake of carbon liquid was prepared in a stainless-steel bowl with flake of carbon/water/sodium-based surfactant addition ratio of 1/45/0.45. Then, the ultrasonic horn stirrer applies a distribution process for the aforementioned suspension constituent at 60 min and 48 W power level. When it needs, the stainless-steel bowl is cooled in a container

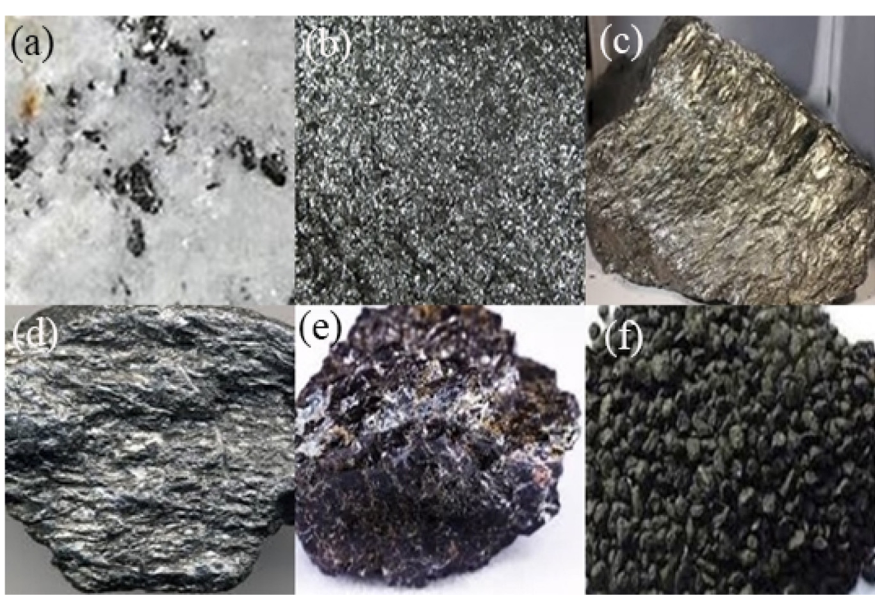

Fig. 3 – (a) The graphite in construction metamorphic and igneous stone; (b) the flake of graphite; (c) the amorphous graphite; (d) the graphite occurred in the hydrothermal process; (e) the graphite in melted rocks and meteoroids; and (f) the artificial graphite.

Table 1 – The descriptive characteristic properties of flake of carbon.

Property	Flake of carbon
Transparency	Opaque
Color from surrounding of graphite	Black
Brightness	Metallic
Color	Steel grey to black
Chemical element	C
Class of Chemical Structure	Native element
Occurrence of planar surface	Perfect
Crystal System	Hexagonal
Specific Gravity	2.1 to 2.3
Mohs Hardness	1 to 2

containing ice so that the suspension could not be affecting the heat negatively. Before mixing of the liquid into the composites of plaster and grout, the colloid flake of carbon suspension is spun for centrifuging at 7500 rpm to keep the flake of carbon dispersed into the liquid.

2.1.2.1. *Characterization of the colloid flake of carbon with spectroscopy*. The absorption spectra of optical atomic equipment which measures the flake mass of carbon in each suspension via vacuum filtration determines the degree of dispersing for the flake of carbon in the ultra-sonication process. To better express the success of dispersing degree, the absorption spectra of colloid flake of carbon is relatively compared to the absorption spectra of colloid flake of carbon measured by an UV-Vis-NIR spectrophotometer each other. Moreover, Table 2 compares the results before and after centrifugation, and it presents the wavelength and the absorption spectra of colloid flake of carbon.

Between the non-centrifuged absorption of 1.209870577 and the centrifuged absorption of 0.001892135, it is clearly observed that the absorption spectra of the concentrated colloid flake of carbon is over six hundred thirty-nine times higher than that of non-concentrated colloid flake of carbon (Table 2). This means that there is not loss on mass of the flake of carbon in the centrifuged liquid.

Table 2 – Comparison of the absorption results before and after centrifugation.

Flake of Carbon Dispersion with centrifugation Wavelength (nm)	Absorption Degree	Flake of Carbon Dispersion without centrifugation Wavelength (nm)	Absorption Degree
900	0.001892135	900	0.602268338
899	0.001914729	899	0.602882803
898	0.002278079	898	0.603197634
897	0.001943772	897	0.603546679
896	0.001986807	896	0.604034662
895	0.002029171	895	0.604338884
894	0.001929705	894	0.604641438
.[a]	.[a]	.[a]	.[a]
.	.	.	.
.	.	.	.
352	0.034421008	352	1.203085661
351	0.034842342	351	1.206427097
350	0.034849327	350	1.209870577

[a] The full stop (.) in the Table 2 stands for continue of the wavelengths and the absorptions between 894 (nm) and 350 (nm) and 0.001929705 and 1.209870577 respectively.

2.1.3. *Pulverized fuel ash of class C*

The power plants and the super power plants originate the pulverized fuel ash of class C from subbituminous coal and lignite coal, and because of its chemical features, it is sorted as artificial pozzolana by ASTM (Fig. 1) [3]. Chemical feature of pulverized fuel ash of class C is greater silicon oxide and aluminum oxide and ferrite oxide, which their total quantity is more than over 65%, and lower loss on ignition (LOI) compared to the pulverized fuel ash of class F [3]. Table 3 compares the chemical properties of pulverized fuel ash of class C with the required chemical properties designated by the ASTM C 618 [24] and BS EN 197-1 [25].

Table 4 presents the required physical and mechanical properties of pulverized fuel ash adhesive suggested by ASTM C 618 [24] and BS EN 197-1 [25].

The pulverized fuel ash of class C could be used as substitution material for adhesive in plaster, grout, concrete, and stucco, the quantity of substitution varies 20–35% of the mass of adhesive [4,12,13,18,25]. Since it is substituted with adhesive, the pulverized fuel ash of class C provides some advantages for adhesive and adhesive based material as follow:

- The compressive strength is increased after 90 days,
- As the pulverized fuel ash of class C is added to adhesive more than 15%, it increases durability properties of adhesive, e.g., resistance of alkali silica reaction (ASR) and of freezing and thawing and of penetration of chlorine ion and of carbonation and of rust.
- The pulverized fuel ash of class C produces lesser heat generation than that of normal adhesive during hydration,
- The pulverized fuel ash of class C increases the compacity of adhesive based materials,
- The pulverized fuel ash of class C decreases the permeability of adhesive based materials,
- The pulverized fuel ash of class C decreases the water demand of adhesive based materials,

Table 3 – Comparison of chemical properties between the pulverized fuel ash of class C and the requirements of ASTM C 618 and BS EN 197-1.

Chemical Properties	Required Chemical Properties of Pulverized Fuel Ash According to ASTM C 618 (%)	Required Chemical Properties of Pulverized Fuel Ash Adhesive According to BS EN 197-1 (%)	Chemical Properties of Pulverized Fuel Ash of Class C used (%)
$SiO_2 + Al_2O_3 + Fe_2O_3$	>50	–	65.5
SO_3	<5	≤3.5	1.7
Loss on ignition (LOI)	<6	≤0.1	0.7

Table 4 – The required physical and mechanical properties of pulverized fuel ash adhesive suggested by BS EN 197-1 and ASTM C 618.

Specifications		The Required physical and mechanical properties of pulverized fuel ash adhesive	
		According to BS EN 197-1	According to ASTM C 618
Soundness (mm)		≤10	–
Compressive strength (MPa)	2 d	>10	–
	28 d	>32.5	≥ (0.85 × 32.5 = 27.6 MPa)
Initial Thickening-time (Vicat test) (min)		>60	–

- The pulverized fuel ash of class C increases the workability of adhesive based materials,
- As the pulverized fuel ash of class C is substituted for adhesive, the pulverized fuel ash of class C decreases $40 per ton for the manufacturing cost of conventional adhesive [4].

If the pulverized fuel ash of class C is used as substitution material for adhesive, it is important to know some disadvantage of the substitution as being follow. The time of thickening may be slightly delayed compared to conventional adhesive. Also, the fine aggregate stack would need to be modified in adhesive based material because the pulverized fuel ash of class C is lower bulk specific gravity than that of conventional adhesive. Therefore, this substitution has to be put higher mass of the pulverized fuel ash of class C to fill same volume in the mixing design of adhesive based material. The pulverized fuel ash of class C must be replaced at least 25% of the adhesive to mitigate harmful effect of alkali silica reaction on adhesive based material. If any organic and inorganic admixture, such as air entrainment, is used in the mixing design of adhesive based material, the substitution amount of pulverized fuel ash of class C for adhesive must be modified since calcium oxide in the pulverized fuel ash of class C adsorbs the organic and inorganic admixture. Finally, if the pulverized fuel ash of class C has high calcium oxide content, it should not be used in sulfate exposure applications because the sulfate environment may easily decompose calcium oxide-based compound, e.g., the portlandite, being in hydration. With using it and/or any other alternative supplementary cementitious material into adhesive and adhesive based material, it is necessary to make trial mixture to ensure proper proportioning for the desired quality [4,12,13,18,24].

2.1.4. *Type I adhesive of ASTM and oil well adhesive*

The type I adhesive of ASTM is described as artificial inorganic mineralogical adhesive material includes major and minor chemical features as 60–70% calcium oxide (CaO), 20–25% silicon oxide (SiO_2), 4–8% aluminum oxide (Al_2O_3), 1–4% ferrite oxide (Fe_2O_3), 0–2% magnesium oxide (MgO), 1–3% sulfur oxide (SO_3), under 1% alkali, and 0–1% loss on ignition [3,4,15,16]. The chemical features reveal that the type I adhesive of ASTM displays regular physical and mechanical properties, e.g., the Portland cement in use in-situ applications of traditional infrastructure and construction.

2.2. *Mixture proportioning, design and manufacturing of ecology-friendly adhesive combination and hydraulic plaster composite and hydraulic grout composite*

Table 5 lists the classes of ecology-friendly adhesive combination, the chemical compositions of type I adhesive of ASTM as control adhesive, new hydraulic adhesive doped flake of

Table 5 – The classes of ecology-friendly adhesive combination, the chemical compositions of type I adhesive of ASTM as control adhesive, new hydraulic adhesive doped flake of carbon, pulverized fuel ash of class C, ecology-friendly adhesive substituted pulverized fuel ash of class C with type I adhesive of ASTM, new green hydraulic adhesive doped flake of carbon, and dosage of adhesive for 1 m^3.

Chemical composition (%)	Type I adhesive of ASTM	New hydraulic adhesive doped flake of carbon		Pulverized fuel ash of class C	New ecology-friendly hydraulic adhesive doped flake of carbon			Adhesive dosage for one cubic meter
		Type I adhesive doped flake of carbon	Type I adhesive doped colloid flake of carbon		Pulverized Fuel Ash of Class C -Adhesive	Pulverized fuel ash of class C-adhesive doped flake of carbon	Pulverized fuel ash of class C- adhesive doped colloid flake of carbon	
CaO	62.9	62.9	62.9	21.3	48.3	48.3	48.3	380
SiO_2	20.2	20.2	20.2	38.4	26.5	26.5	26.5	380
Al_2O_3	4.7	4.7	4.7	21.8	10.6	10.6	10.6	380
Fe_2O_3	3.3	3.3	3.3	5.2	3.9	3.9	3.9	380
MgO	2.7	2.7	2.7	4.4	3.2	3.2	3.2	380
SO_3	3.3	3.3	3.3	1.7	2.7	2.7	2.7	380
Na_2O	–	–	–	1.6	0.5	0.5	0.5	380
K_2O	–	–	–	0.5	0.1	0.1	0.1	380
Flake of carbon	–	0.2	–	–	–	0.2	–	380
Colloid flake of carbon	–	–	0.2	–	–	–	0.2	380
Loss on ignition (LOI)	1.1	1.1	1.1	0.7	0.9	0.9	0.9	380

carbon, pulverized fuel ash of class C, ecology-friendly adhesive substituted pulverized fuel ash of class C with type I adhesive of ASTM, new green hydraulic adhesive doped flake of carbon, and dosage of adhesive for 1 m^3.

To determine the thickening-periods of adhesive combination, the hydraulic plaster composite samples were prepared as described following proportioning for one cubic meter. Hydraulic control plaster composites were prepared with sprinkling water/adhesive ratio of 1/1.3. Hydraulic type I adhesive of ASTM + flake of carbon plaster (P1) composite and hydraulic type I adhesive of ASTM + colloid flake of carbon plaster (P2) composite was prepared with sprinkling water/adhesive/flake of carbon or colloid flake of carbon ratio of 1/1.3/0.0044. Hydraulic type I adhesive of ASTM + pulverized fuel ash of class C ecology-friendly plaster (P3) composites were prepared with sprinkling water/ecology-friendly adhesive ratio of 1/1.3. Hydraulic type I adhesive of ASTM + pulverized fuel ash of class C + flake of carbon ecology-friendly plaster (P4) composite and hydraulic type I adhesive of ASTM + pulverized fuel ash of class C + colloid flake of carbon ecology-friendly plaster (P5) composite was prepared with sprinkling water/new ecology-friendly adhesive/flake of carbon or colloid flake of carbon ratio of 1/1.3/0.0044.

To determine the spreading, consolidating level, and spreading ratio of fresh grout composite and unit volume mass, water adsorption, apparent porosity, apparent compacity, and compressive stress of hardened grout composite, hydraulic grout composite samples were prepared as described following proportioning for one cubic meter. Hydraulic type I adhesive of ASTM as control grout composites were prepared with sprinkling water/adhesive/sand ratio of 1/1.3/6 for one cubic meter. Hydraulic type I adhesive of ASTM + flake of carbon grout (M1) composite and type I adhesive of ASTM + colloid flake of carbon grout (M2) composite was prepared with sprinkling water/adhesive/sand/flake of carbon or colloid flake of carbon ratio of 1/1.3/6/0.0044. Hydraulic type I adhesive of ASTM + pulverized fuel ash of class C ecology-friendly grout (M3) composites was prepared with sprinkling water/adhesive/sand ratio of 1/1.3/6. Hydraulic type I adhesive of ASTM + pulverized fuel ash of class C + flake of carbon ecology-friendly grout (M4) composite and hydraulic type I adhesive of ASTM + pulverized fuel ash of class C + colloid flake of carbon ecology-friendly grout (M5) composite was prepared with sprinkling water/adhesive/sand/flake of carbon or colloid flake of carbon ratio of 1/1.3/6/0.0044.

2.3. Testing procedures

2.3.1. Determining for thickening-time

The thickening time is the term described the hardening period of the fresh adhesive plaster composite because of hydration reactions between water and adhesive, and the Vicat equipment, either automatic one or manual one, determines the initial and final thickening-time of the adhesive plaster composite which is prepared in the Section 2.2 [3,4]. The fresh adhesive plaster composite filled mold is placed on the base-plate in the Vicat equipment in which is a container containing water at 20 ± 3 °C. The Vicat equipment with 1 mm needle is levelled properly until it is in contact top surface of the composite of conventional and ecology-friendly adhesive plaster. The penetration is repeated on different pointing of same specimen at 10 min intervals until the needle sinks no more than 5 mm from the base-plate of the Vicat equipment, and this time of 5-mm-sinking is recorded as the initial thickening-time. When the needle penetrates only 0.5 mm on the top surface of sample, this time together with the time from zero is recorded for the final thickening-time of composite of conventional and ecology-friendly adhesive plaster [3,4,24].

2.3.2. Determining for spreading, consolidating level, and spreading ratio

A spreading table equipment, either automatic or manual, determines the measure of spreading, which describes the spreading of fresh phase of adhesive grout composite and ecology-friendly adhesive grout composite, and the spreading ratio and consolidating level of fresh adhesive grout composites prepared as Section 2.2 being. How to test the composites with the spreading table is as following enumerating being. First, a layer of fresh grout composite with 25-mm-high is put in the mold, and it is tampered 20 times with hand tamper. Then, the mold is fully filled with fresh grout and tampered as specified for the first layer. The fully filled mold is lifted on the spread table, and it is immediately dropped 25 times in 15 s unless otherwise specified [3,4]. There is a need for measuring the consolidating level and the spreading ratio of fresh phase of adhesive grout composite and of green adhesive grout composite. Following calculations cope with the demands. The spread ratio is a measuring the determined spreading to the dimension of mold. However, the consolidating level is a measuring the difference of fresh phase of grout composite in heights between the molded composite and the spreaded composite.

2.3.3. Determining for unit volume mass

The unit volume mass testing is performed with some laboratory tools such as a digital weighing scale which has a precision of 0.01 g, LCD digital vernier caliper, and a digital furnace which could dry plenty of much sample at the same time. Before the testing, the sample of control grout composite and of the green adhesive grout composite is dried by furnace at 105 ± 5 °C until each one shows constant mass. The constant mass of grout composite sample is designated by the digital weighing scale, and it is recorded as W_d (g). Volume for the sample of grout composite is measured by the LCD digital vernier caliper, and it is recorded as V_d (cm^3). The unit volume mass (d) is calculated by W_d/V_d as (gcm^{-3}) [26,27]. Average of eighteen-unit volume masses quantity specifies the descriptive unit volume mass for both control grout composite and grout composite doped flake of carbon/colloid flake of carbon and green adhesive grout composite doped flake of carbon/colloid flake of carbon in Table 6 and following figures.

2.3.4. Determining for water adsorption

The test laboratory unit has to be a standard condition which is less than 0.2 m/s speed of air and at 90 ± 5% relative humidity for 7-day to measure the water adsorption property. After provided the standard condition for laboratory, the water

Table 6 – The classes of ecology-friendly adhesive plaster composite, the classes of ecology-friendly adhesive grout composite, and their properties.

Testing		Conventional adhesive Plaster	Conventional adhesive plaster doped flake of carbon and colloid flake of carbon		Ecology-friendly adhesive plaster	Ecology-friendly adhesive plaster doped flake of carbon and colloid flake of carbon	
		Control	P1	P2	P3	P4	P5
Thickening-Period	Initial (min)	125	[a]Cx0.72	[a]Cx0.88	[a]Cx1.93	[a]Cx1.84	[a]Cx1.68
	Final (min)	210	[a]Cx0.71	[a]Cx1	[a]Cx1.68	[a]Cx1.62	[a]Cx1.47

Types of Testing		Conventional adhesive grout		Conventional adhesive superior grout doped flake of carbon and colloid flake of carbon				Ecology-friendly adhesive grout		Ecology-friendly adhesive superior grout doped flake of carbon and colloid flake of carbon			
		Control	Standard deviation	M1	Standard deviation	M2	Standard deviation	M3	Standard deviation	M4	Standard deviation	M5	Standard deviation
Spreading (mm)		165	0.02	[a]Cx0.88	0.01	[a]Cx0.85	0.06	[a]Cx1.13	0.03	[a]Cx1	0.05	[a]Cx1.01	0.07
Spreading ratio (%)		206.25	0.03	181.25	0.07	175	0.02	232.5	0.04	206.2	0.01	208.7	0.03
Consolidating level (mm)		30	0.01	18	0.04	15	0.08	41	0.02	30	0.03	32	0.02
Unit volume mass (g/cm^3)		1.87	0.05	2.01	0.03	1.94	0.03	2.06	0.01	2.07	0.06	2.06	0.02
Apparent porosity (%)		12.5	0.03	11.5	0.01	11	0.02	7.6	0.05	10.2	0.03	10.8	0.02
Apparent compacity (%)		87.5	0.06	88.5	0.05	89	0.07	92.4	0.09	89.8	0.08	89.2	0.03
Water adsorption (%)		11.17	0.04	10.33	0.02	9.91	0.01	7.06	0.05	9.29	0.03	9.74	0.06
Compressive stress (MPa)	1-d	3.35	0.06	[a]Cx1.107	0.01	[a]Cx1.38	0.05	[a]Cx1.27	0.03	[a]Cx1.11	0.08	[a]Cx1.46	0.02
	2-d	4.61	0.01	[a]Cx 1.11	0.02	[a]Cx1.26	0.07	[a]Cx2.02	0.01	[a]Cx1.75	0.03	[a]Cx1.89	0.05
	3-d	7.72	0.02	[a]Cx 1	0.03	[a]Cx1.04	0.04	[a]Cx1.38	0.05	[a]Cx1.18	0.04	[a]Cx1.31	0.01

Types of testing		Class of oil well adhesive suggested by API	
		G	H
Compressive stress (MPa)	1-d at 15.5 °C-water curing	3.03	2.2
	1-d at 26.6 °C-water curing	8.1	7.3
	1-d at 35 °C-water curing and 5.5 MPa atmospheric pressure	17.5	14.5
Thickening-period (min)	Initial	Between 90 and 120	

[a] C stands for the abbreviation of Control in the Table 6.

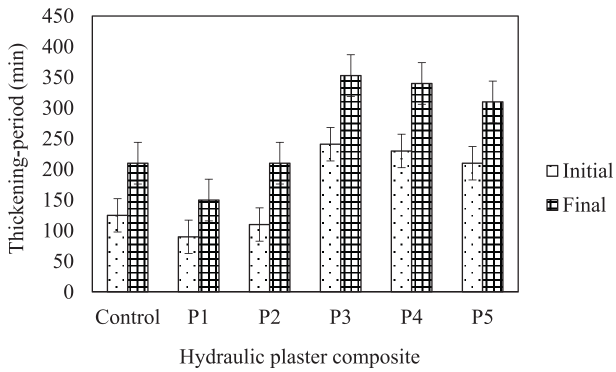

Fig. 4 – The comparison of the initial and final thickening-periods between the examined plaster composite of regular conventional adhesive and plaster composite of conventional adhesive doped flake of carbon and colloid flake of carbon and plaster composite of ecology-friendly adhesive doped flake of carbon and colloid flake of carbon.

adsorption test of the hardened grout is performed as being in the following procedure with using a humidity controlled curing cabinet for 7-day:(1) mix grout as proportioned in the Section 2.2; (2) after 1-day casting of grout, immerse the hardened-grout into 20 ± 3 °C water in humidity controlled curing cabinet; (3) add 20 ± 3 °C water to maintain the water level constant when necessary; (4) pull out grout from water curing at 7-day; (5) weigh the water-absorbed-hardened grout and record its water-absorbed-mass as m_t; (6) place the water-absorbed-hardened grout in a furnace at 50 ± 5 °C; (7) desiccate the water-absorbed-hardened grout until it achieves the constant weigh; (8) weigh the desiccated-hardened grout and record its desiccated-mass as m_d; (9) compute the water adsorption of grout (W_{wa}) according to Eq. (1);

$$W_{wa} = m_t - m_d(\%) \tag{1}$$

(10) examine the water adsorption with three samples for each grout batch [26,27]. Table 6 presents the average of water adsorption of eighteen samples as descriptive water adsorption for both control grout composite and grout composite doped flake of carbon/colloid flake of carbon and green adhesive grout composite doped flake of carbon/colloid flake of carbon.

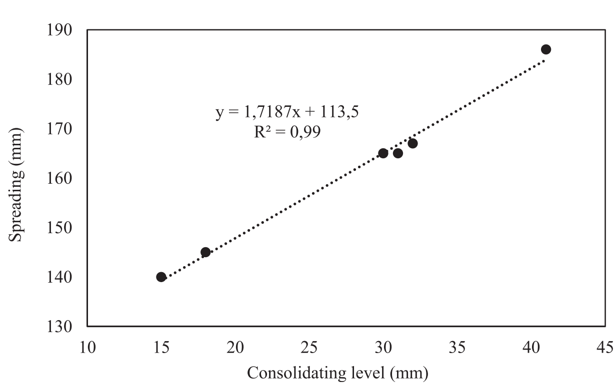

Fig. 5 – The particle packing linear model for the fresh state of grout composite of conventional adhesive and grout composite of hydraulic ecology-friendly adhesive doped flake of carbon and colloid flake of carbon.

2.3.5. *Determining for apparent porosity*

The apparent porosity test is performed with some laboratory tools such as a water curing cabinet, digital weighing scale which has a precision of 0.01 g, and a digital furnace which could dry plenty of much sample at the same time. Before the test, the sample of green grout composite is dried by furnace at 105 ± 5 °C until each one shows constant mass. The constant mass of the sample of grout composite and of green adhesive grout composite is designated by the digital weighing scale, and it is recorded as (W_d) (g). Then, the sample is placed in water curing cabinet, and sprinkling water is put to cover up to 50 (mm) high on top surface of the sample. After 24 h, the digital weighing scale measures the first wet mass of the sample. This wet weighing measurement process is continued until it demonstrates no 1% difference between last and current measurements, and the constant current water saturated measurement of grout is recorded as ultimate wet mass (W_w) (g). Lastly, the water absorbed-hardened grout is immersed in the volume-levelled-water to measure the displaced water level as (W_{ws}). The apparent porosity (P) is calculated According to Eq. (2) [26,27].

$$P = \left(\frac{W_w - W_d}{W_w - W_{ws}}\right) \cdot 100(\%) \tag{2}$$

Average of eighteen apparent porosities quantity specifies the descriptive apparent porosity for both control grout composite and grout composite doped flake of carbon/colloid flake of carbon and green adhesive grout composite doped flake of carbon/colloid flake of carbon in Table 6 and following figures.

2.3.6. *Determining for apparent compacity*

The apparent compacity (C) is calculated according to Eq. (3) [26,27].

$$C = 100 - P(\%) \tag{3}$$

Average of eighteen apparent compacities quantity specifies the descriptive apparent compacity for both control grout composite and grout composite doped flake of carbon/colloid flake of carbon and green adhesive grout composite doped flake of carbon/colloid flake of carbon in Table 6 and following figures.

2.3.7. *Determining for compressive stress*

Mechanical axial compression force testing evaluates the fundamental compressive stress of control grout composite and of grout composite doped flake of carbon/colloid flake of carbon and of green adhesive grout composite doped flake of carbon/colloid flake of carbon as proportioned in the Section 2.2. The testing is carried out with fifty-four samples in a closed-loop MTS servo-hydraulic testing machine with a 110 kip (489 kN) capacity with the compression force loading rate of 0.008 mm/min. Average of the compressive stress specifies the descriptive compressive stress for both control grout composite and grout composite doped flake of carbon/colloid flake of carbon and green adhesive grout composite doped flake of carbon/colloid flake of carbon in Table 3 and following figures [26,27]. The compressive stress which is known force to area is calculated by Eq. (4)

$$R_c = \frac{F}{2580.6} \cdot (N/mm^2)$$

where R_c is the compressive stress; F_c is maximum compression force up to fracture.

3. Physico-mechanical properties and mathematical models for the PEA

Table 6 summarizes the classes of ecology-friendly adhesive plaster composite, the classes of ecology-friendly adhesive grout composite, the thickening-time of adhesive plaster composite, the spreading, the spreading ratio, and the consolidating level of fresh state of ecology-friendly adhesive grout composite, the unit volume mass, the water adsorption, the apparent porosity, and the apparent compacity of ecology-friendly adhesive grout composite hardened, and the compressive stress of ecology-friendly adhesive grout composite hardened.

Additionally, the figures set up meaningful relationships between properties determined in the following sections. In the section, the readers would also understand how the flake of carbon and the colloid flake of carbon influence on the constructional properties of plain hydraulic adhesive plaster and grout, hydraulic adhesive of pulverized fuel ash of class C, ecology-friendly plaster and superior grout composite in term of performance effect assessment, e.g., specification of adhesive and of oil well adhesive, durability, and strength related property.

3.1. *Thickening–period*

Fig. 4 shows the comparison of the initial and final thickening-periods between the examined plaster composite of regular conventional adhesive and plaster composite of conventional adhesive doped flake of carbon and colloid flake of carbon and plaster composite of ecology-friendly adhesive doped flake of carbon and colloid flake of carbon. This figure presents that the thickening-period is shortened by the colloid flake of carbon. The most impressive result related to the ecology-friendly hydraulic adhesive of pulverized fuel ash of class C is that the blended colloid flake of carbon definitely gets the P5 plaster composite of ecology-friendly adhesive up 21 min earlier than the P3 plaster composite of ecology-friendly adhesive, and the stiffness of P5 occurs 43 min early than that of P3. The result could be attributed that the increased dormant period, which is caused by the 35% replacement of pulverized fuel ash of class C with conventional adhesive is handled by doping both flake of carbon and colloid flake of carbon (Table 6 and Fig. 4).

Sample called the P1, adhesive plaster composite doped only 1 g flake of carbon, displays the shortest thickening-period in the plaster composites. A similar supportive result, like the P1 composites being, is reached for thickening-period in the plaster composites of ecology-friendly hydraulic adhesive including pulverized fuel ash of class C and flake of carbon and colloid flake of carbon (Table 6 and Fig. 4). This means that the flake of carbon and the colloid flake of carbon ease to shorten the increased period of thickening in the plaster composite of ecology-friendly hydraulic adhesive. Its reason is possibly due to the high activation effect of flake of carbon and colloid flake of carbon on the calcium oxide in which is high content in the pulverized fuel ash of class C and conventional type I adhesive of ASTM. Similarly, this high accelerator effect of flake of carbon and colloid flake of carbon could handle to reduce the increased thickening-period in the oil well adhesive and in the hydraulic ecology-friendly adhesive of pulverized fuel ash of class C whose calcium oxide (CaO) content is more than 10%. The P1 and P2 is the most suitable conventional hydraulic adhesive doped 0.22% flake of carbon and/or colloid flake of carbon and included 100% type I adhesive of ASTM for oil well constructing according to their thickening-period. The thickening occurs among ninety and one hundred 10 min in the P1 and the P2. This period makes the P1 and the P2 favorable adhesive plasters for oil well application. Results of thickening-period indicates that small addition of flake of carbon and/or colloid flake of carbon significantly increases the hydration rate of both conventional type I adhesive of ASTM and ecology-friendly hydraulic adhesive. The analysis of achieved data indicates that the particle packing ability of flake of carbon and of colloid flake of carbon on the thickening-period reported for grout composite is diversified and it reduces initial and final period of thickening along with helping the covalent bonding of carbon–carbon in the mineralogical supplement in use. In the presence of weak bonding of hydrogen in adhesive based construction material, the individual particle packing ability of 1 g-flake of carbon and of 1 g-colloid flake of carbon is a shortener of the thickening-period for both conventional grout composite of hydraulic adhesive and grout composite of hydraulic

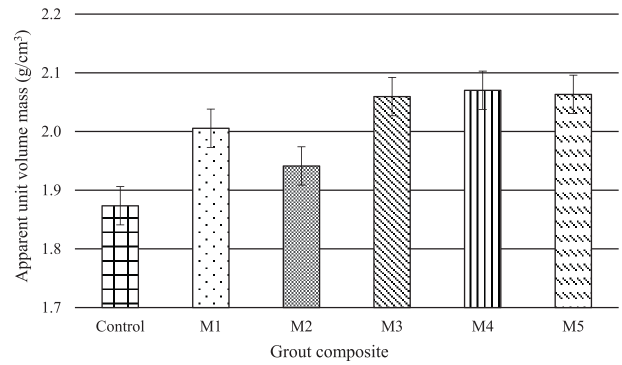

Fig. 6 – The particle packing effect of flake of carbon and colloid flake of carbon doping on the unit volume mass for the hardened state of grout composite of hydraulic ecology-friendly adhesive and grout composite of conventional adhesive.

ecology-friendly adhesive because those, may be, form a kind of the hydro-carbon (H–C), which is one of the most known molecular bonding, through hydration products, e.g., the C–S–H gel, the CH, and the C-A-H, in the grout as being in the bonding structure of plastic, rubber, and fiber.

3.2. Spreading, spreading ratio, and consolidating level

Fig. 5 shows the particle packing linear model for the fresh state of conventional grout composite of adhesive and grout composite of hydraulic ecology-friendly adhesive doped flake of carbon and colloid flake of carbon. The packing and spreading of fresh state of conventional adhesive grout and hydraulic ecology-friendly adhesive grout are influenced by the particle packing ability directly. This means that the particle packing can be managed by the particle-size distribution of adhesive in composite used in the applications of construction and infrastructure. For that aim, the particle packing is significant to all adhesive system in a fluid medium, it changes fresh state of adhesive composite from plastic to solid.

The adhesive powder cannot fill the voids better than optimum level defined by the particle-size gradation in a material based on time depended hardness process. Proper gradation system which could fill voids each other can control to manage the maximum particle packing in all size, millimeter to nano, and can be used to improve rheological and workability issues for superior material. The Fig. 5 contains a linear formula, whose r^2 is very close to 1, and an r square for relationship degree between spreading and consolidating level. It specifies that the decreasing of consolidating level is result of the decreasing of spreading (Fig. 5). As the solid-to-liquid phase ratio varies in a narrow range of percent among 7.3 and 8, the particle packing occurs in optimum level. Moreover, it is obvious that the flow decreases since the solid-to-liquid phase ratio increases, and flake of carbon and colloid flake of carbon increased causes coagulation for mixtures of grout composite of conventional adhesive and grout composite of hydraulic ecology-friendly adhesive (Table 6 and Fig. 5). The highest reduction in the spreading, spreading ratio, and consolidating level is in the M2 grout composite that was made of conventional type I adhesive of ASTM and colloid flake of carbon. The ratio of 0.022-colloid flake of carbon-to-water reduces, respectively, the spreading, spreading ratio, and consolidating level of M2 grout composite more than over 15%, 17.5%, and 50% compared to the control grout composite. The highest growth in the spreading, spreading ratio, and consolidating level is in the M3 that is made of 35%-pulverized fuel ash of class C that is geometrical shape of sphere and 65% conventional type I adhesive of ASTM because it contains neither the flake of carbon nor the colloid flake of carbon. Substitution of pulverized fuel ash of class C for conventional type I adhesive of ASTM increases, respectively, the spreading, spreading ratio, and consolidating level of M3 ecology-friendly grout composite more than over 13%, 12.7%, and 36% compared to the control grout composite (Table 6 and Fig. 5). Therefore, the performance effect assessment of the pulverized fuel ash of class C is a spreading increaser mineralogical artificial pozzolana for doping and replacement of hydraulic ecology-friendly adhesive in engineering application. Compared to that of M3 ecology-friendly adhesive grout composite, the spreading, spreading ratio, and consolidating level of M4 is equal, and that of M5 green grout composite is over 1%, 1.1%, and 6.5% greater, respectively, since the flake of carbon and the colloid flake of carbon are put in the M4 and M5 separately (Table 6 and Fig. 5). However, compared to that of control grout composite, the spreading, spreading ratio, and consolidating level of M1 and of M2 composite is over 12% and 15% lower, over 13.7% and 17.8% lower, and 40% and 50% lower, respectively, since the flake of carbon and the colloid flake of carbon are put in the M1 and M2 separately (Table 6 and Fig. 5). The results imply that both the flake of carbon and the colloid flake of carbon decreases ability of spreading in both grout composite of conventional hydraulic adhesive and grout composite of hydraulic ecology-friendly adhesive. However, the use of flake of carbon and colloid flake of carbon shows such a benefit as reducing of the plasticity, which could help packing the conventional hydraulic adhesive and conformity the pulverized fuel ash of class C with conventional adhesive, in order to shorten the thickening-period of adhesive and the demolding duration in construction application. Moreover, the best doping material for both the conventional

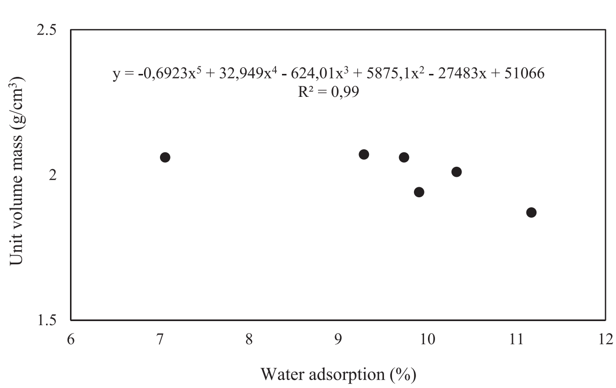

Fig. 7 – A fifth-degree equation between unit volume mass and water adsorption of the hardened conventional grout composite and ecology-friendly grout composite doped flake of carbon and colloid flake of carbon.

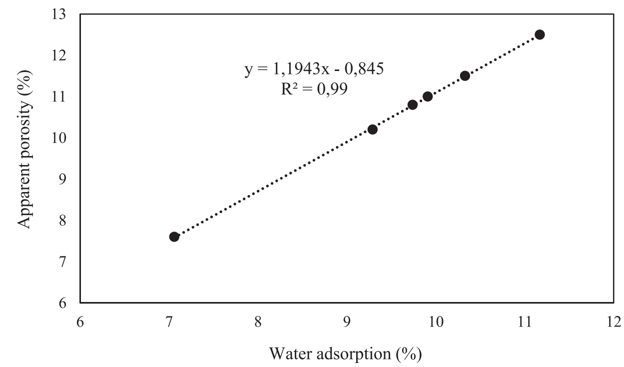

Fig. 8 – A linear model between apparent porosity and water adsorption of the hardened conventional grout composite and ecology-friendly grout composite doped flake of carbon and colloid flake of carbon.

hydraulic adhesive and the hydraulic ecology-friendly adhesive composite is the colloid flake of carbon because it does not need to absorb water from the mixing of grout composite and does not affect their workability feature negatively.

3.3. *Apparent unit volume mass*

Fig. 6 presents the particle packing effect of flake of carbon and colloid flake of carbon doping on the unit volume mass for the hardened state of grout composite of hydraulic ecology-friendly adhesive and grout composite of conventional adhesive. Scientific research related to grout made with conventional adhesive and ecology-friendly adhesive reports that the wet curing is necessary process for the unit volume mass of ecology-friendly hydraulic grout composite as well as strength development. The unit volume mass is also influenced by other main factors of mixture and proportion of grout composite e.g., size of fine sand, quantity of fine sand, liter of mixing water, loss on mixing water and fine adhesive plaster through evaporation, and vibration method in use [20].

Decisive average unit volume mass measured from the hardened grout composite of M1 and M2 is 1.97 g cm^{-3} that is over 5% greater than that of control grout composite (Table 6 and Fig. 6). The average unit volume mass measured from the hardened ecology-friendly hydraulic grout composite of M3, M4, and M5 is 2.06 g/cm^3 that is 10% higher than that of control grout composite (Table 6 and Figs. 6 and 7). However, Fig. 7 gives a fifth-degree equation between unit volume mass and water adsorption of the hardened conventional grout composite and ecology-friendly grout composite doped flake of carbon and colloid flake of carbon.

Fig. 7 also contains the formula of equation, whose r^2 is very close to 1, and the r square is a forceful indicator for the presence of relationship and the degree of relationship. It specifies that the increasing of unit volume mass depends on the particle packing ability of flake of carbon and colloid flake of carbon (Figs. 6 and 7). In the light of results, according to the performance effect assessment, it is obvious that both the flake of carbon and the colloid flake of carbon has particle packing effect as increaser for the unit volume mass of ecology-friendly grout composite and conventional grout composite. This could be closely related to two new bonding structures which are known as the bonding of carbon–carbon and of hydro-carbon caused by the doping of flake of carbon and colloid flake of carbon.

3.4. *Apparent porosity*

Fig. 8 renders a linear model between apparent porosity and water adsorption of the hardened conventional grout composite and ecology-friendly grout composite doped flake of carbon and colloid flake of carbon. This figure also contains the linear formula, whose r^2 is very close to 1, and the r square is a forceful indicator for the presence of relationship and the degree of relationship. It specifies that the decreasing of apparent porosity depends on particle packing ability of the flake of carbon and the colloid flake of carbon (Fig. 8).

The most impressive result relates to the decrease in apparent porosity of M3 ecology-friendly grout composite made with 35% the pulverized fuel ash of class C and 65% type I adhesive of ASTM because the pulverized fuel ash of class C has an ability to make chemical reaction with conventional adhesive to enhance the portlandite formed in hydration process (Table 6). Decisive average apparent porosity of the ecology-friendly grout composite of M3, M4, and M5 is 9.5% that is over 31.5% lower than that of control grout composite (Table 6). Therefore, the M3, M4, and M5 absorb lower water than both regular grout composite of conventional adhesive and grout composite of conventional adhesive doped flake of carbon and colloid flake of carbon. Another decisive average apparent porosity measured from the composite of hardened conventional hydraulic grout of M1 and M2 is 11.2% that is over 11.6% lower than that of control grout composite. The quantity of apparent porosity is the expected minimum porosity for the composite of conventional and ecology-friendly grout hardened. This could be due to the particle packing ability of flake of carbon and colloid flake of carbon on the apparent porosity reported for the grout composites. In other words, individual particle packing ability of flake of carbon and colloid flake of carbon on the apparent porosity of composite of conventional grout of M1 and M2 is, respectively, over 8.6% and 13.6% higher than that of control grout

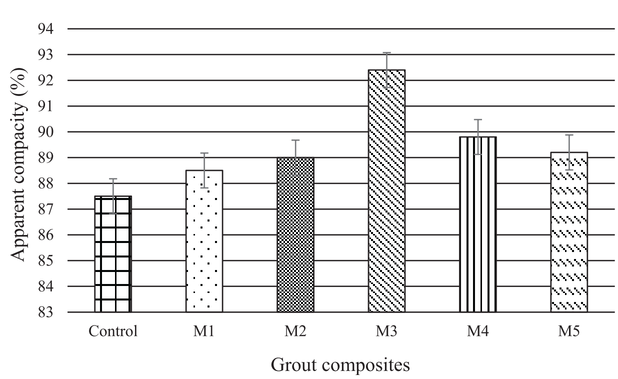

Fig. 9 – The particle packing effect of flake of carbon and colloid flake of carbon doping on the apparent compacity of hydraulic ecology-friendly adhesive grout and conventional adhesive grout.

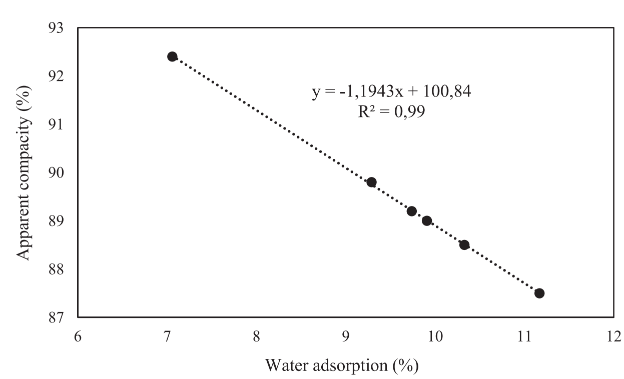

Fig. 10 – A linear model for the particle packing ability of flake of carbon and colloid flake of carbon doping on the apparent compacity for the hardened composite state of ecology-friendly hydraulic grout and conventional composite of adhesive grout.

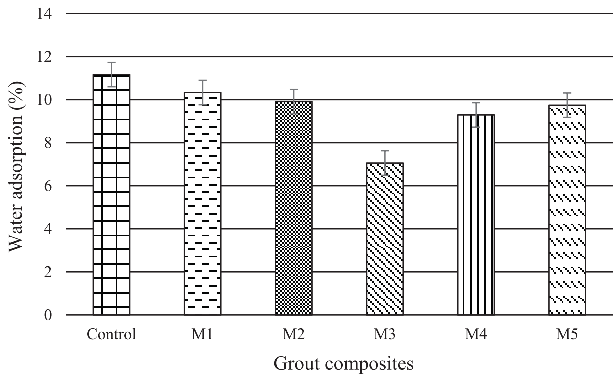

Fig. 11 – The particle packing effect of flake of carbon and colloid flake of carbon doping on the water adsorption for the hardened state of ecology-friendly grout composite and conventional grout composite.

composite (Table 6). A similar result can be seen in the composite of M4 and M5 green grout. The individual particle packing ability of flake of carbon and colloid flake of carbon on the apparent porosity of composite of ecology-friendly grout of M4 and M5 is, respectively, over 22.5% and 15.7% higher than that of control grout composite. One can point from the apparent porosity result that owing to doping the 1 g-flake of carbon for the composite of hydraulic conventional adhesive grout and the composite of hydraulic ecology-friendly adhesive grout, the flake of carbon reduces the apparent porosity is as 8.6% for M1 and 22.5% for M4 along with artificial pozzolanic effect of pulverized fuel ash of class C. Similar to the previous argument, doping of the colloid flake of carbon reduces the apparent porosity is as 13.6% for M2 and 15.7% for M5 along with pulverized fuel ash of class C (Table 6). According to performance effect assessment, this is obvious that main ability of both flake of carbon and colloid flake of carbon has a reducer of apparent porosity for conventional composite of hydraulic adhesive grout and ecology-friendly composite of hydraulic adhesive grout.

3.5. *Apparent compacity*

Fig. 9 renders the particle packing effect of flake of carbon and colloid flake of carbon doping on the apparent compacity of

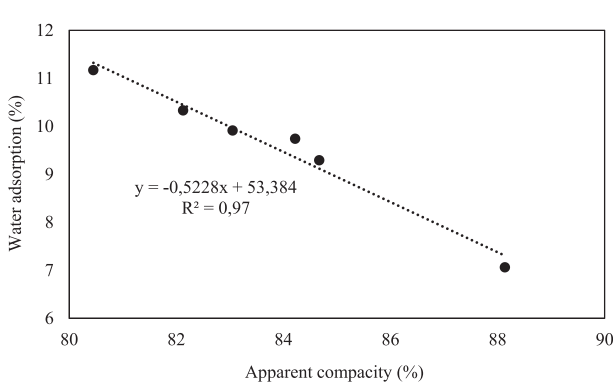

Fig. 12 – A linear equation between the water adsorption and the apparent compacity of hardened grout composite doped flake of carbon and colloid flake of carbon.

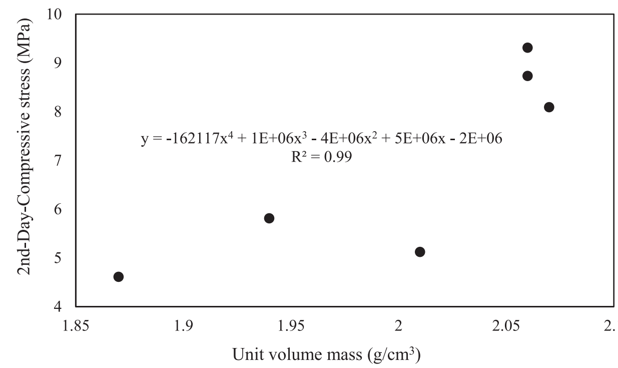

Fig. 13 – A fourth-degree equation between the 2nd-day compressive stress and unit volume mass of hardened conventional grout composite and ecology-friendly grout composite doped flake of carbon and colloid flake of carbon.

composites of hydraulic ecology-friendly adhesive grout and conventional adhesive grout. Compared to the apparent compacity in the composites studied, the apparent compacity of M3 ecology-friendly grout composite is also the highest because the M3 contains 65% type I adhesive of ASTM and 35% pulverized fuel ash of class C. The apparent compacity of control grout composite is the lowest since the composite of control grout does not contain neither the pulverized fuel ash of class C, the flake of carbon nor the colloid flake of carbon (Table 6 and Fig. 9).

The average apparent compacity of the ecology-friendly grout composite of M3, M4, and M5 is 90.5% that is over 3.4% greater than that of control grout composite (Table 6). Therefore, the M3, M4, and M5 absorb lower water than both the composite of hydraulic grout doped flake of carbon and colloid flake of carbon and the composite of control grout. The average apparent compacity measured from the composite of hardened hydraulic grout of M1 and M2 is 88.7% that is over 1.3% lower than that of control grout composite. This quantity of apparent compacity is the expected maximum apparent compacity for the composite of conventional and ecology-friendly grout hardened. This could be due to the particle packing ability of flake of carbon and of colloid flake of carbon on the apparent compacity reported for the grout composites. In other words, individual particle packing ability of flake of carbon and of colloid flake of carbon on the apparent compacity of conventional grout composite of M1 and M2 is, respectively, over 1.1% and 1.7% lower than that of control grout composite (Table 6). A similar result can be seen in the composite of M4 and M5 ecology-friendly adhesive grout. The individual particle packing ability of flake of carbon and of colloid flake of carbon on the apparent compacity of the composite of ecology-friendly grout of M4 and M5 is, respectively, over 2.6% and 1.9% greater than that of control grout composite. One could point from the apparent compacity result that owing to doping the 1 g-flake of carbon for the composite grout of hydraulic conventional adhesive and the composite grout of hydraulic ecology-friendly adhesive, the flake of carbon increases the apparent compacity is as 1.1% for M1 and 2.6% for M4. Similar to the previous argument, the doping of

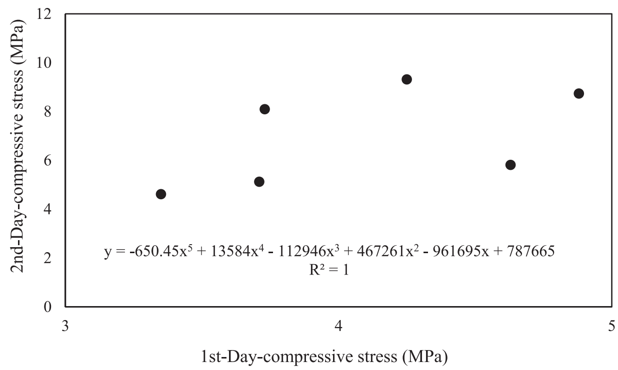

Fig. 14 – A fifth-degree relationship between 1st-day-compressive stress and 2nd-day-compressive stress determined from the grout composites hardened.

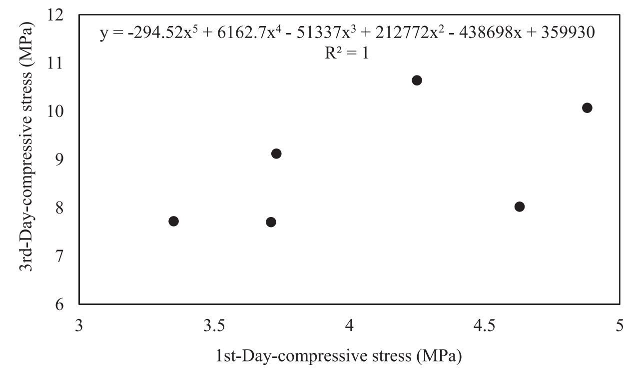

Fig. 15 – A fifth-degree equation between 1st-day-compressive stress and 3rd-day-compressive stress determined from the grout composites hardened.

colloid flake of carbon reduces the apparent compacity is as 1.7% for M2 and 1.9% for M5 (Table 6). Fig. 10 renders a linear model for the particle packing ability of flake of carbon and colloid flake of carbon doping on the apparent compacity for the hardened composite state of ecology-friendly hydraulic grout and conventional composite of adhesive grout. This figure contains a linear equation, whose r^2 is 1, and this r square is a forceful indicator for relationship between the apparent compacity and the water adsorption.

It specifies that the increasing of apparent compacity depends on the particle packing ability of flake of carbon and colloid flake of carbon for the hardened state of composite of hydraulic ecology-friendly adhesive and of conventional composite of hydraulic adhesive (Figs. 9 and 10). According to performance effect assessment, this is obvious that main ability of both the flake of carbon and the colloid flake of carbon has an increaser of apparent compacity for the grout composite of hydraulic conventional adhesive and the grout composite of hydraulic ecology-friendly adhesive.

3.6. *Water adsorption*

Fig. 11 renders the particle packing effect of flake of carbon and colloid flake of carbon doping on the water adsorption for the hardened composite state of ecology-friendly grout and conventional grout composite. Decisive average water adsorption measured from the hardened grout composite of M1 and of M2 is 10.12% that is over 10.3% lower than that of control grout composite. Another decisive average water adsorption measured from the hardened grout composite of ecology-friendly hydraulic adhesive of M3, M4, and M5 is 8.6% that is 29% lower than that of control grout composite (Table 6 and Fig. 11). However, Fig. 12 gives a linear equation between the water adsorption and the apparent compacity of hardened grout composite doped flake of carbon and colloid flake of carbon. Fig. 12 also contains a linear formula of equation, whose r^2 is very close to 1, and the r square is a forceful indicator for the degree of relationship.

The research results allow to conclude that grout composite which is having higher unit volume mass shows lower water adsorption (Table 6, Figs. 11, and 12). The water adsorption of ecology-friendly adhesive grout doped flake of carbon and colloid flake of carbon is nearly over 30% lower than the water adsorption of regular conventional adhesive grout and conventional adhesive grout doped flake of carbon and colloid flake of carbon.

High differences in water adsorption, even up to 30%, are noticed in case of flake of carbon and colloid flake of carbon having extreme quality (Figs. 11 and 12). In the light of results, according to the performance effect assessment, it is obvious that low water adsorption does not cause problems regarding on efflorescence, alkali–silica reaction, and harmful chemical minerals coming from earth. The flake of carbon and colloid flake of carbon seems to be profitably technological treatment especially for application of conventional adhesive grout and ecology-friendly adhesive grout having lower water adsorption, containing lower mineral adhesive fraction, and having greater compression strength.

3.7. *Compressive stress development*

Fig. 13 presents a fourth-degree equation between the 2nd-day compressive stress and unit volume mass of hardened conventional grout composite and ecology-friendly grout composite doped flake of carbon and colloid flake of carbon, including the compressive stress the curing age of 2 days and grout diversity.

This figure also contains the formula of fourth-degree equation and the r square is a forceful indicator for the degree of relationship between the unit volume mass and the compressive stress. It specifies that the increasing of compressive stress is result of the increasing of unit volume mass and particle packing ability of flake of carbon and colloid flake of carbon for the hardened state of ecology-friendly adhesive grout composite and conventional adhesive grout composite (Fig. 13). At both 1 day and 3 days, the highest strength is determined in M5 ecology-friendly adhesive grout composite because it contains the amount of pulverized fuel ash of class C to a maximum of 205 kg and the amount of type I adhesive of ASTM to a maximum of 380.8 kg and the amount of colloid flake of carbon to a maximum of 2.6 kg and the amount of sand to a maximum of 1757.8 kg per cubic meter (Table 6). At first day, compressive stress of grout composite of M1 with flake of carbon and M2 with colloid flake of carbon is, respectively, over 8% and 35% greater than that of control grout composite. The ecology-friendly grout composite of M3 with only pulverized fuel ash of class C, M4 with flake of carbon, and M5 with colloid flake of carbon also shows over 23%, 8%, and 41% higher compressive stress compared to control grout composite (Table 6 and Fig. 13). Fig. 14 presents a fifth-degree relationship between 1st-day-compressive stress and 2nd-day-compressive stress determined from the grout composites hardened.

This study also reveals that while the artificial pozzolanic effect of pulverized fuel ash of class C provides over 23.5% greater compressive stress for type I adhesive of ASTM, the particle packing ability of flake of carbon and colloid flake of carbon provides, respectively, over 8% and 35% higher compressive stress for grout composite of conventional adhesive at the ages of 1 days. Fig. 14 also contains the fifth-degree equation, and the r square is a forceful indicator for the degree of relationship between 1st-day-compressive stress and 2nd-day-compressive stress. There is available to predict the 2nd-day-compressive stress from 1st-day-compressive stress in the broad stress range of 3 and 10 MPa through Fig. 14. It specifies that the increasing of compressive stress is result of the particle packing ability of flake of carbon and colloid flake of carbon for the grout composites of ecology-friendly adhesive and conventional adhesive (Fig. 14). Whereas the combination of particle packing ability of pulverized fuel ash of class C and flake of carbon is over 8% growth for compressive stress development, the combination of particle packing ability of pulverized fuel ash of class C and colloid flake of carbon is over 40% raising for compressive stress development in the grout composite of conventional adhesive at the age of 1 days (Table 6 and Figs. 13 and 14). At the curing age of 2 days, compressive stress related to M1 with flake of carbon and M2 with colloid flake of carbon is, respectively, over 10% and 26% greater than that of control grout composite. The ecology-friendly grout composite of M3 with only pulverized fuel ash of class C, M4 with flake of carbon, and M5 with colloid flake of carbon also present similar strength growth, like M1 and M2 at the age of 2 days. Those growing are respectively over 202%, 73%, and 89% greater compressive stress compared to control grout composite (Table 6). This study reveals that whereas single effect of pulverized fuel ash of class C provides over two times greater compressive stress for the grout composite of conventional adhesive, single effect of flake of carbon and colloid flake of carbon is, respectively, over 10.5% and 26% higher compressive stress for the grout composite of conventional adhesive at the age of 2 days. Whereas the combination of artificial pozzolanic effect of pulverized fuel ash of class C and particle packing ability of flake of carbon is over 74% growth for compressive stress development, the combination of artificial pozzolanic effect of pulverized fuel ash of class C and particle packing ability of colloid flake of carbon is over 89% raising for compressive stress development for the grout composite of conventional adhesive at the curing age of 2 days. Fig. 15 presents a fifth-degree equation between 1st-day-compressive stress and 3rd-day-compressive stress determined from the grout composites hardened.

Fig. 15 also contains the fifth-degree equation, and the r square is a forceful indicator for the degree of relationship between 1st-day-compressive stress and 3rd-day-compressive stress. There is available to predict the 3rd-day-compressive stress from 1st-day-compressive stress in the narrow stress range of 7 and 11 MPa through Fig. 15. It specifies that the increasing of compressive stress is result of the particle packing ability of flake of carbon and colloid flake of carbon for the conventional grout composite hardened (Table 6 Fig. 15). After the curing age of 3 days, compressive stress of M1 grout composite with flake of carbon shows the same stress development of control grout composite, and compressive stress of M2 grout composite with colloid flake of carbon is over 3% greater than that of control grout composite. The M3 ecology-friendly grout composite with only pulverized fuel ash of class C, M4 ecology-friendly grout composite with pulverized fuel ash of class C and flake of carbon, and M5 ecology-friendly grout composite with pulverized fuel ash of class C and colloid flake of carbon also demonstrate, respectively, over 24%, 18%, and 29% higher compressive stress development compared to control grout composite with only conventional adhesive, sand, and sprinkled water (Table 6 and Fig. 15). This study also reveals that whereas single artificial pozzolanic effect of pulverized fuel ash of class C provides over 24.5% greater compressive stress for conventional grout composite, the particle packing ability of colloid flake of carbon renders over 3.5% higher compressive stress for conventional grout composite at the age of 3 days. Whereas the combination of artificial pozzolanic effect of pulverized fuel ash of class C and particle packing ability of flake of carbon is over 18% growth for compressive stress development, the combination of artificial pozzolanic effect of pulverized fuel ash of class C and particle packing ability of colloid flake of carbon is over 29.5% raising for compressive stress development in conventional grout composite at the curing age of 3 days. In the light of results, according to the performance effect assessment, both conventional adhesive grout and ecology-friendly grout composite needs doping the flake of carbon and colloid flake of carbon to be able to be widely used in engineering applications, such as super tall building, super concrete, and infrastructure.

4. Conclusion

Results support following conclusions:

- The particle packing ability of flake of carbon and colloid flake of carbon is a thickening accelerator in thickening-period, an increaser in apparent density and apparent compacity, and reducer in spreading and apparent porosity as well as developer in compressive stress at the ages of 1 days, 2 days, and 3 days. In the light of results and conclusions, the use of flake of carbon and colloid flake of carbon is necessary for developing the properties of new ecology-friendly grout composite and conventional grout composite. Plus, those using is, especially, necessary for conventional adhesive and ecology-friendly adhesive by means of particle packing property, rapid thickening, and compressive stress development.

- In view of positive properties of flake of carbon and colloid flake of carbon, those could be used such construction engineering applications as ecology-friendly construction and infrastructure building, infrastructure renewal, construction retrofit, and construction reinforcement.
- As explained in the article, colloid flake of carbon is the best doping material, and renders logical, productive, and sustainable development in the properties of conventional grout composite and ecology-friendly grout composite for saving the future of conventional and ecology-friendly adhesive and construction application.

Data availability statement

The research data used to support the findings of this study are available from the corresponding author upon request.

Declaration of Competing Interest

The authors declare that they have no known competing financial interests or personal relationships that could have appeared to influence the work reported in this paper.

Acknowledgments

Corresponding author declares that this studying does not include any research budget obtained from either non-profit organization and/or profit organization.

REFERENCES

[1] Cahen D, Lubomirsky I. Energy, the global challenge, and materials. Mater Today 2008;11(12):16–20. https://doi.org/10.1016/S1369-7021(08)70248-7.
[2] Lee B. Opinion: the waste problem? Mater Today 2006;9(3):64. https://doi.org/10.1016/S1369-7021(06)71423-7.
[3] Kırgız MS. Advance treatment by nanographite for Portland pulverised fly ash cement (the class F) systems. Compos B Eng 2015;82:59–71. https://doi.org/10.1016/j.compositesb.2015.08.003.
[4] Kırgız MS. Green cement composite concept reinforced by graphite nano-engineered particle suspension for infrastructure renewal material. Compos B Eng 2018;154:423–9. https://doi.org/10.1016/j.compositesb.2018.09.012.
[5] Mani S, Pradhan B. Investigation on effect of fly ash content on strength and microstructure of geopolymer concrete in chloride-rich environment. Mater Today: Proceedings 2020;32(Part 4):865–70. https://doi.org/10.1016/j.matpr.2020.04.216.
[6] Das SK, Shrivastava S. A study on the viability of fly ash and construction and demolition waste as geopolymerized masonry mortar and their comparative analysis. Mater Today: Proceedings 2020;32(Part 4):574–83. https://doi.org/10.1016/j.matpr.2020.02.402.
[7] Kumar BP, Francis RR, Raouf A, Subramanian R, Gupta S, Kannan G, et al. Torrefied materials derived from waste vegetable biomass. Mater Today: Proceedings 2020;28(Part 2):852–5. https://doi.org/10.1016/j.matpr.2019.12.311.
[8] Devi BM, Chore HS. Feasibility study on bagasse ash as light weight material for road construction. Mater Today: Proceedings 2020;27(Part 2):1668–73. https://doi.org/10.1016/j.matpr.2020.03.568.
[9] Andavan S, Pagadala VK. A study on soil stabilization by addition of fly ash and lime. Mater Today: Proceedings 2020;22(Part 3):1125–9. https://doi.org/10.1016/j.matpr.2019.11.323.
[10] Wang H, Feng Q, Tang X, Liu K. Preparation of high-purity graphite from a fine microcrystalline graphite concentrate: effect of Alkali roasting pre-treatment and acid leaching process. Separ Sci Technol 2016;51(14):2465–72. https://doi.org/10.1080/01496395.2016.1206933.
[11] Kundanati RR, Malpani T, Sairam V. Study on mechanical properties of mortar using alccofine and graphene oxide. Mater Today: Proceedings 2020;22(Part 4):2431–8. https://doi.org/10.1016/j.matpr.2020.03.369.
[12] Meng W, Khayat KH. Mechanical properties of ultra-high-performance concrete enhanced with graphite nanoplatelets and carbon nanofibers. Compos B Eng 2016;107(12):113–22. https://doi.org/10.1016/j.compositesb.2016.09.069.
[13] Meng W, Khayat KH. Effect of graphite nanoplatelets and carbon nanofibers on rheology, hydration, shrinkage, mechanical properties, and microstructure of UHPC. Cement Concr Res 2018;105(3):64–71. https://doi.org/10.1016/j.cemconres.2018.01.001.
[14] Hung P, Lau K, Fox B, Hameed N, Lee JH, Hui D. Surface modification of carbon fibre using graphene-related materials for multifunctional composites. Compos B Eng 2018;133:240–57. https://doi.org/10.1016/j.compositesb.2017.09.010.
[15] Wosu SN, Hui D, Daniel L. Hygrothermal effecs on the dynamic compressive properties of graphite/epoxy composite. Mater Compos Part B: Eng 2012;43(3):841–55. https://doi.org/10.1016/j.compositesb.2011.11.045.
[16] Ahmad H, Fan M, Hui D. Graphene oxide incorporated functional materials. Compos B Eng 2018;145(6):270–80.
[17] Liu S, Chevali SV, Xu Z, Hui D, Wang H. A review of extending performance of epoxy resins using carbon materials. Compos B Eng 2018;136:197–214. https://doi.org/10.1016/j.compositesb.2017.08.020.
[18] Peyvandi A, Soroushian P, Farhadi N, Balachandra AM. Evalution of the reinforcement efficiency of low-cost graphite nanomaterials in high-performance concrete. KSCE J Civil Eng 2018;22(10):3875–82. https://doi.org/10.1007/s12205-018-0168-6.
[19] Singh N, Hui D, Singh R, Ahuja IPS, Feo L, Fraternali F. Recycling of plastic solid waste: a state of art review and future applications. Compos B Eng 2017;115:409–22. https://doi.org/10.1016/j.compositesb.2016.09.013.
[20] Ngo TD, Kashani A, Imbalzano G, Nguyen KTQ, Hui D. Additive manufacturing (3D Printing): a review of materials, methods, applications and challenges. Compos B Eng 2018;143:172–96. https://doi.org/10.1016/j.compositesb.2018.02.012.
[21] Colangelo F, Russo P, Cimino F, Cioffi R, Farina I, Fraternali F, et al. Epoxy/glass fibres composites for civil applications: comparison between thermal and microwave crosslinking routes. Compos B Eng 2017;126:100–7. https://doi.org/10.1016/j.compositesb.2017.06.003.

[22] Campbell QC, editor. Graphite: properties, occurrences and uses. 1st. New York: Nova Science Publishers Incorporated; 2013.

[23] Chang LLY. Industrial mineralogy: materials, processes, and uses. 1st. Upper Saddle River: Prentice-Hall; 2002.

[24] American Society of Testing and Materials. ASTM C 61-19 – standard specification for coal fly ash and raw or calcined natural pozzolan for use in concrete. 2019. p. 1–5.

[25] [a]. British Standards Institution. BS EN 197-1:2011 – cement composition, specifications and conformity criteria for common cements. 2019. p. 1–56.
[b]. Meng T, Yu Y, Wang Z. Effect of nano-$CaCO_3$ slurry on the mechanical properties and micro-structure of concrete with and without fly ash. Compos B Eng 2017;117:124–9. https://doi.org/10.1016/j.compositesb.2017.02.030.

[26] Kırgız MS. Advancements in Mechanical and physical properties for marble powder–cement composites strengthened by nanostructured graphite particles. Mech Mater 2016;92:223–34. https://doi.org/10.1016/j.mechmat.2015.09.013.

[27] Kırgız MS. Nanosize particle packing for nanoconcretes and cement based materials: mathematical models, theory, and technology. In: Liew MS, Nguyen-Tri P, Nguyen TA, Kakooei S, editors. Smart nanoconcretes and cement-based materials – properties, modelling, and applications. 1st. Oxford: Elsevier; 2020.